

**Figure 1.** The normalized current  $I/I_0$  as a function of  $a = p/q$  at  $\tilde{\nu} = 0.2$  for different Landau–Zener tunneling amplitudes,  $\tau$ .  $I_0 = |e|\Delta/\hbar$ . Arrows indicate the positions of maxima.

$\delta\varphi \ll 2\pi\nu t_0$ . Note that the inequality  $\nu t_0 \ll 1$  is essential for maintaining a significant energy pumping.

Another approximation is that we have allowed for relaxation in the simplest possible way by using a single relaxation time in the equation for the density matrix. This assumption is adequate if the relaxation is caused by a transfer of the electrons in *real space* between the ring and a surrounding reservoir. If the electron energy spectrum in the reservoir is continuous, then the lifetime of an electron state in the ring with respect to this mechanism is almost independent of its quantum numbers. The mechanism discussed above allows us to describe electron states in the ring as pure quantum states, the relaxation rate being the decay through escape to the reservoir. The exact results obtained above are relevant for the case when such an ‘escape’ mechanism dominates. Internal inelastic relaxation processes in the ring can in principle lead to a significant difference between phase- and energy relaxation rates. Such a situation requires a separate treatment. However, in the most interesting case of efficient Landau–Zener tunneling, the intrinsic inelastic processes must involve a large momentum transfer and therefore they are strongly suppressed [5].

In conclusion, the quantum electron dynamics problem in a single-channel ballistic ring with a barrier, subjected to a linearly time-dependent magnetic flux has been solved exactly. Exponential localization in energy space has been proven. Finally, we have shown that the dc-current exhibits a set of peaks with fractional structure when plotted as a function of the induced electro-motive force. This structure is strongly sensitive to the barrier height, as well as to the relaxation rate.

**Acknowledgments.** This work was supported by KVA, TFR and the Research Council of Norway. We also acknowledge partial financial support from INTAS (Grant No. 94-3862).

## References

1. Imry Y, in *Quantum Coherence in Mesoscopic Systems* (NATO ASI Series B: Physics, Ed. B Kramer) (New York: Plenum, 1991) Vol. 254
2. Büttiker M, Imry Y, Landauer R *Phys. Lett. A* **96** 365 (1983); Landauer R *Phys. Rev. B* **33** 6497 (1986)
3. Gefen Y, Thouless D J *Phys. Rev. Lett.* **59** 1752 (1987)

4. Gefen Y, Thouless D J *Phil. Mag. B* **56** 1005 (1987)
5. Swahn T et al. *Phys. Rev. Lett.* **73** 162 (1994)
6. Shimshoni E, Gefen Y *Ann. Phys. (N.Y.)* **210** 16 (1991)
7. Hübner R, Graham R *Phys. Rev. B* **53** 4870 (1996)
8. Casati G et al., in *Stochastic Behavior in Classical and Quantum Hamiltonian Systems, Volta Memorial Conference, Como, Italy, 1997* (Lecture in Physics, Vol. 93, Eds G Casati, J Ford) (Berlin, New York: Springer-Verlag, 1979) p. 334; Gempel DR, Prange RE, Fishman S *Phys. Rev. A* **29** 1639 (1984)
9. Blatter G, Browne D A *Phys. Rev. B* **37** 3856 (1988)
10. Ao P *Phys. Rev. B* **41** 3998 (1990)
11. Landau L D *Phys. Zs. Sowjetunion* **2** 46 (1932); Zener C *Proc. R. Soc. London A* **137** 696 (1932); Mullen K et al. *Phys. Rev. Lett.* **62** 2543 (1989)
12. Gorelik L et al., submitted to *Phys. Scr.*

## Interference effects in mesoscopic disordered rings and wires

M Pascaud, G Montambaux

### 1. Introduction

The observation of persistent currents in mesoscopic metallic rings has revived interest in the comprehension of interference effects in coherent diffusive systems [1–5] (for a review and additional references see Ref. [6]). While transport quantities like the weak-localization correction were calculated in the ’80s, the persistent current was studied more recently with the same techniques [7–17]. All these quantities can be related to Diffuson or Cooperon diagrams which describe the diffusive nature of the electronic motion, when the mean free path  $l_c$  is shorter than the typical size  $L$  of the system.

These diagrammatic calculations were then rewritten in a more transparent way which explicitly relates the quantities of interest to the return probability for a diffusive particle. In this paper, we summarize the derivation of these quantities, using a formalism which very simply relates all the quantities and which allows their calculation from the knowledge of a single function. We have recently used this formalism to calculate the mesoscopic magnetization in various geometries like connected rings. This may give a better understanding of the experimental situation as well as of the interplay between interaction and disorder in mesoscopic structures [15]. As examples, we present here the results for rings and wires which can be derived straightforwardly from this formalism.

### 2. Transport, thermodynamics and return probability

We characterize the diffusive motion by the quantity  $p_\gamma(\mathbf{r}, \mathbf{r}', t)$ , solution of the diffusion equation:

$$\left[ \frac{\partial}{\partial t} + \gamma - D \left( \nabla + \frac{2ie\mathbf{A}}{\hbar c} \right)^2 \right] p_\gamma(\mathbf{r}, \mathbf{r}', t) = \delta(\mathbf{r} - \mathbf{r}')\delta(t), \quad (1)$$

where  $D$  is the diffusion coefficient. The scattering rate  $\gamma = D/L_\phi^2$  describes the breaking of phase coherence.  $L_\phi$  is the phase coherence length.  $\gamma$  will be compared to  $1/\tau_D = D/L^2$  where  $\tau_D$  is the diffusion time, i.e. the typical time to diffuse through a system of size  $L$ . This time is the inverse of the Thouless energy  $E_c = \hbar D/L^2$ .

The return probability is actually the sum of two terms, a purely classical one and an interference term which results from interferences between pairs of time-reversed trajectories. In the diagrammatic picture, they are related to the Diffuson and Cooperon diagrams. The interference term,  $p_\gamma^C(\mathbf{r}, \mathbf{r}', t)$ , is field dependent and is a solution of the above equation. The classical term,  $p_\gamma^D(\mathbf{r}, \mathbf{r}', t)$ , is field independent. It is a solution of the above equation with  $\mathbf{A} = 0$ . Since the two functions have the same form, we use the same notation  $p_\gamma(\mathbf{r}, \mathbf{r}', t)$  for Diffuson and Cooperon contributions.

The diffusion equation has to be completed by appropriate boundary and continuity equations. In the general case of a non-translation invariant geometry, the return probability  $p_\gamma(\mathbf{r}, \mathbf{r}, t)$  depends on the starting point  $\mathbf{r}$ . One important quantity is the space-integrated return probability defined as

$$P_\gamma(t) = \int d\mathbf{r} p_\gamma(\mathbf{r}, \mathbf{r}, t).$$

We also recall the expression of the Cooperon  $C_\gamma(\mathbf{r}, \mathbf{r})$  — whose zero field expression also corresponds to the Diffuson at any field<sup>†</sup>:

$$C_\gamma(\mathbf{r}, \mathbf{r}) = \int_0^\infty dt p_\gamma(\mathbf{r}, \mathbf{r}, t).$$

It turns out that all the transport and thermodynamical quantities of interest can be related to time integrals of  $P_\gamma(t)$ . We now review these quantities.

It has been shown in previous works [16, 17] that the weak-localization correction to the conductivity  $\sigma$  can be written in terms of the interference part of the return probability:

$$\langle \delta\sigma \rangle = -2s \frac{e^2 D}{h\Omega} \int P_\gamma(t) dt,$$

where  $\Omega$  is the volume,  $s$  is the spin degeneracy. In the case of a wire, the correction to the dimensionless conductance  $g = G/(e^2/h)$  is thus

$$\langle \delta g \rangle = -2s \int P_\gamma(t) \frac{dt}{\tau_D},$$

where  $\tau_D = L^2/D$  is the diffusion time through the wire.

Similarly, the conductivity fluctuation can be written directly as a function of  $P_\gamma(t)$  [6, 15, 18]. When time-reversal symmetry (TRS) is broken (large magnetic field), it is given by

$$\langle \delta\sigma^2 \rangle = 12s^2 \left( \frac{e^2 D}{h\Omega} \right)^2 \int t P_\gamma(t) dt,$$

so that, in the wire geometry, the conductance fluctuation is

$$\langle \delta g^2 \rangle = 12s^2 \int P_\gamma(t) \frac{t dt}{\tau_D^2}.$$

In the more general case where the field  $H$  is finite,  $P_\gamma(t)$  should be replaced by  $P_\gamma(t, 0) + P_\gamma(t, H)$ .

<sup>†</sup> The lower bound of the time integrals in this paper is actually the mean collision time  $\tau_c$  above which diffusion takes place.

We now turn to spectral and thermodynamic quantities. The number variance  $\Sigma^2(E)$  measures the fluctuation of the number of energy levels in a fixed energy range of size  $E$ . It is an integral of the two-point correlation function of the density of states whose Fourier transform, the form factor, can be semiclassically related to the return probability  $P_\gamma(t)$  [11]. As a result, the number variance can be written directly as an integral of  $P_\gamma(t)$ :

$$\Sigma^2(E) = \frac{2s^2}{\pi^2} \int_0^\infty \frac{P_\gamma(t)}{t} \sin^2 \frac{Et}{2} dt,$$

when TRS is broken. Like for the conductance fluctuations,  $P_\gamma(t)$  should be replaced by  $P_\gamma(t, 0) + P_\gamma(t, H)$  in a finite field. This expression is a semiclassical result: the region where  $E$  becomes as small as the level spacing  $\Delta$ , corresponding to times  $t$  as large as the Heisenberg time  $h/\Delta$  is not well described.

In the presence of a magnetic field  $H$ , the mesoscopic magnetization of a ring or a more general network is characterized by its average and typical values. The typical value can also be related to the two-point correlation of the density of states [6, 11] and then to  $P_\gamma(t)$ . At zero temperature, it is (taking the spin into account):

$$M_{\text{typ}}^2(H) = \frac{1}{2\pi^2} \int_0^\infty \frac{P_\gamma''(t, H)|_0^H}{t^3} dt,$$

where  $P_\gamma''(t, H)|_0^H = \partial^2 P_\gamma / \partial H^2|_H - \partial^2 P_\gamma / \partial H^2|_0$ ;  $H$  is the magnetic field.

The main contribution to the average magnetization comes from the Hartree–Fock correction to the energy [9, 12]. It can be rewritten in terms of the two-point correlation function of the local density of states and then in terms of the return probability [14]:

$$\langle M_{\text{cc}} \rangle = -\frac{U\rho_0}{\pi} \frac{\partial}{\partial H} \int_0^\infty \frac{P_\gamma(t, H)}{t^2} dt,$$

where  $U$  is the screened Coulomb interaction;  $\rho_0$  is the density of states, where  $U = 4\pi e^2/q_{\text{TF}}^2$  (higher order corrections have been considered in Ref. [19]);  $q_{\text{TF}}$  is the Thomas–Fermi vector.

One sees that all these physical quantities are time integrals of the return probability with various power-law weighting functions. Noting that  $P_\gamma(t)$  has the form  $P_0(t) \exp(-\gamma t)$ , all these quantities can be written as integrals or derivatives with respect to  $\gamma$  of a single function  $S(\gamma, H)$  that we call the *spectral function*:

$$S(\gamma, H) = \int \frac{P_0(t, H)}{t} \exp(-\gamma t) dt = \int_\gamma^\infty d\gamma \int C_\gamma(\mathbf{r}, \mathbf{r}, H) d\mathbf{r}. \quad (2)$$

This function  $S$  is related to the logarithm of the spectral determinant defined in Ref. [20]. The number variance for a closed system can be written in terms of this function

$$\Sigma^2(E) = \frac{2s^2}{\beta\pi^2} \text{Re}[S(\gamma) - S(\gamma + iE)], \quad (3)$$

where  $s$  is the spin degeneracy;  $\beta = 1$  with TRS;  $\beta = 2$  if TRS is broken.

The different magnetizations can be given in terms of the successive integrals of this function:

$$\langle M_{ee}(H) \rangle = -\frac{U\rho_0}{\pi} \frac{\partial}{\partial H} S^{(1)}(\gamma, H), \quad (4)$$

$$M_{\text{typ}}^2(H) = \frac{1}{2\pi^2} \frac{\partial^2}{\partial H^2} S^{(2)}(\gamma, H)|_0^H, \quad (5)$$

where  $S^{(n)}(\gamma) = \int_{\gamma_1}^{\infty} d\gamma_n \dots \int_{\gamma_2}^{\infty} d\gamma_1 S(\gamma_1)$ .

Similarly, the weak-localization correction is easily written as a function of  $S(\gamma)$ :

$$\langle \delta\sigma \rangle = 2s \frac{e^2 D}{h\Omega} \frac{\partial S}{\partial \gamma}. \quad (6)$$

And finally, the conductivity fluctuation is also simply related to  $S$ . For pure symmetries, one has:

$$\langle \delta\sigma^2 \rangle = \frac{24s^2}{\beta} \left( \frac{e^2 D}{h\Omega} \right)^2 \frac{\partial^2 S}{\partial \gamma^2}. \quad (7)$$

### 3. Solution of the diffusion equation on a network

In principle, the calculation of these quantities is now straightforward since it only requires the solution of the diffusion equation for the system being considered. The case of networks made of quasi-1D wires is simple, because the diffusion can be described as one-dimensional. It was considered by Doucot and Rammal for the calculation of weak-localization corrections [17]. Here we generalize it to all transport and thermodynamic quantities. The Cooperon  $C_\gamma(r, r')$  obeys the one-dimensional diffusion equation

$$\left[ \gamma - D \left( \nabla + \frac{2ieA}{\hbar c} \right)^2 \right] C_\gamma(r, r') = \delta(r - r') \quad (8)$$

with the continuity equations written for every node  $\alpha$  (including the starting point  $r'$  that can be considered as an additional node in the lattice) [17]:

$$\sum_{\beta} \left( -i \frac{\partial}{\partial r} + \frac{2eA}{\hbar c} \right) C_\gamma(r, r')|_{r=\alpha} = \frac{i}{DS} \delta_{r',\alpha}, \quad (9)$$

$r, r'$  are linear coordinates on the network;  $S$  is the section of the wire. The sum is taken over all links relating the node  $\alpha$  to its neighboring nodes  $\beta$ . Integration of the differential equation (8) with the boundary conditions (9) leads to the so-called network equations which relate  $C_\gamma(\alpha, r')$  to the neighboring  $C_\gamma(\beta, r')$ :

$$\begin{aligned} \sum_{\beta} \coth \left( \frac{l_{\alpha\beta}}{L_\phi} \right) C(\alpha, r') - \sum_{\beta} \frac{C(\beta, r') \exp(-i\gamma_{\alpha\beta})}{\sinh(l_{\alpha\beta}/L_\phi)} \\ = \frac{L_\phi}{DS} \delta_{\alpha, r'}, \end{aligned} \quad (10)$$

where  $l_{\alpha\beta}$  is the length of the link  $(\alpha\beta)$ , and

$$\gamma_{\alpha\beta} = \frac{4\pi}{\phi_0} \int_{\alpha}^{\beta} \mathbf{A} \cdot d\mathbf{l}$$

is the circulation of the vector potential along this link. Solving this set of linear equations and performing a spatial integration of  $C_\gamma(r', r')$  give access to the spectral function.

## 4. Examples

We now consider the cases of wires and rings of length  $L$ . In this case the physical quantities can be written as a function of the dimensionless function  $S(x)$ :

$$S(x) = \int \frac{P(t)}{t} \exp \left( -x \frac{t}{\tau_D} \right) dt, \quad (11)$$

where  $x = \hbar\gamma/E_c = \gamma\tau_D = (L/L_\phi)^2$ . The magnetization  $M$  of a ring is proportional to its persistent current  $I = M/A$ , where  $A$  is the area of the ring. We have

$$\begin{aligned} \langle \delta g \rangle &= 2s S'(x), \\ \langle \delta g^2 \rangle &= \frac{24s^2}{\beta} S''(x), \\ \Sigma^2(E) &= \frac{2s^2}{\beta\pi^2} \text{Re} \left[ S(x) - S \left( x + \frac{iE}{E_c} \right) \right], \\ \langle I_{ee} \rangle &= -\frac{U\rho_0}{\pi} \frac{e}{\tau_D} \frac{\partial}{\partial \varphi} S^{(1)}(x, \varphi), \\ I_{\text{typ}}^2 &= \frac{1}{2\pi^2} \left( \frac{e}{\tau_D} \right)^2 \frac{\partial^2}{\partial \varphi^2} S^{(2)}(x, \varphi)|_0^\varphi, \end{aligned} \quad (12)$$

where  $S^{(n)}(x)$  are integrals of  $S$  with respect to  $x$ , and  $\varphi$  is the magnetic flux in units of the flux quantum  $\Phi_0 = h/e$ . It is important to note that the cut-offs may be different for the different quantities considered [21]. However, this does not modify the functional relations we have found.

### 4.1 Isolated wire

We first consider the case of an isolated wire. Since no current can flow at the edges, the boundary conditions are:

$$\frac{\partial}{\partial r} C(r, r')|_0 = \frac{\partial}{\partial r} C(r, r')|_L = 0.$$

Integration of the differential equation with these boundary conditions gives [17]:

$$C(r, r) = \frac{L_\phi}{D} \cosh \left( \frac{r}{L_\phi} \right) \cosh \left( \frac{L-r}{L_\phi} \right) \left[ \sinh \left( \frac{L}{L_\phi} \right) \right]^{-1}.$$

After spatial integration and integration with respect to the cut-off, the spectral function  $S$  is found to be

$$S(x) = -\ln \sqrt{x} \sinh \sqrt{x}.$$

Using Eqns (12) the spectral rigidity can be derived. From the expansion of the spectral function

$$\ln \sqrt{x} \sinh \sqrt{x} = \ln x + \sum_{n>0} \ln \left( 1 + \frac{x}{\pi^2 n^2} \right), \quad (13)$$

one recovers the expansion of the variance number in diffusion modes given by Alsthuler and Shklovskii for the 1D case [22].

### 4.2 Connected wire

We now consider the case of a wire perfectly connected to external leads. Using the boundary condition  $C(0, r') = C(L, r')$ , one has [17]

$$C(r, r) = \frac{L_\phi}{D} \sinh \left( \frac{r}{L_\phi} \right) \sinh \left( \frac{L-r}{L_\phi} \right) \left[ \sinh \left( \frac{L}{L_\phi} \right) \right]^{-1}.$$

The spectral function  $S$  is now

$$S(x) = -\ln \frac{\sinh \sqrt{x}}{\sqrt{x}} = -\sum_{n>0} \ln \left( 1 + \frac{x}{\pi^2 n^2} \right). \quad (14)$$

The logarithmic contribution of the zero mode in Eqn (13) is suppressed. The weak-localization correction and the variance of the conductance fluctuations can be found immediately using expressions (12). In particular, in the limit of complete phase coherence  $L_\phi \gg L$ , i.e.  $x \rightarrow 0$ , the expansion of the function  $S(x)$ ,

$$S(x) \rightarrow -\frac{x}{6} + \frac{x^2}{180},$$

immediately leads to the known universal values, for  $s = 1$  and broken TRS:

$$\begin{aligned} \langle \delta g \rangle &= 2S'(0) = -\frac{1}{3}, \\ \langle \delta g^2 \rangle &= 12S''(0) = \frac{2}{15}. \end{aligned}$$

The variance should be multiplied by two when there is time reversal symmetry. When  $L_\phi$  is finite, the variance of the fluctuations is simply related to the mean weak-localization correction ( $s = 1$ ):

$$\langle \delta g^2 \rangle = -12 \frac{\partial}{\partial x} \langle \delta g \rangle, \quad (15)$$

where  $\langle \delta g \rangle = 1/x - \coth \sqrt{x}/\sqrt{x}$ . The size dependence of the conductance fluctuation is shown in Fig. 1. For large samples, it has the expected  $(L/L_\phi)^3$  behavior, with a prefactor quite different from that usually used in the literature [23]. Former experimental results and estimates of  $L_\phi$  should be reconsidered in the light of our result.

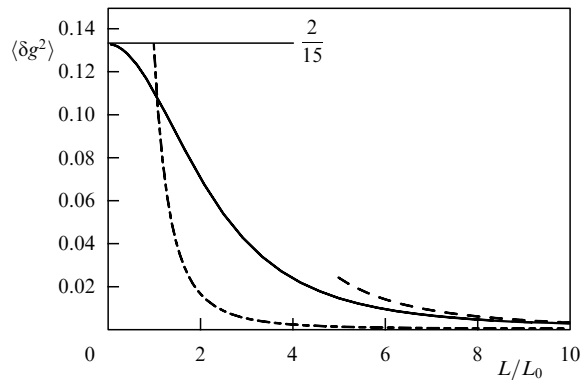


**Figure 1.** Size dependence of the conductance fluctuations for a wire of length  $L$ . The full line represents the result of our calculation. The dash-dotted line shows the expansion used in the literature  $(2/15)(L/L_\phi)^3$ , and the dotted line shows the actual asymptotic behavior  $3(L/L_\phi)^3$ .

### 4.3 Ring

In the case of a ring of perimeter  $L$ , the Cooperon is now translation invariant:

$$C(r, r) = \frac{L_\phi}{2D} \frac{\sinh(L/L_\phi)}{\cosh(L/L_\phi) - \cos(4\pi\varphi)},$$

so that

$$S(x, H) = -\ln [\cosh \sqrt{x} - \cos(4\pi\varphi)]. \quad (16)$$

We deduce immediately the weak-localization correction:

$$\langle \delta g \rangle = -\frac{1}{\sqrt{x}} \frac{\sinh \sqrt{x}}{\cosh \sqrt{x} - \cos(4\pi\varphi)}.$$

From derivation with respect to  $x$ , one obtains a simple but lengthy expression for  $\langle \delta g^2 \rangle$ . It agrees with that calculated by Aronov and Sharvin in the form of an infinite sum over diffusion modes [24].

The average persistent current is

$$\langle I_{ec} \rangle = U\rho_0 \frac{e}{\tau_D} \int_x^\infty \frac{\sin(4\pi\varphi)}{\cosh \sqrt{x} - \cos(4\pi\varphi)} dx. \quad (17)$$

This integral can be calculated explicitly in terms of the Lobatchevskii function and it has the Fourier decomposition found by Ambegaokar and Eckern [12].

The typical persistent current is given by Eqns (12) and agrees with previous calculations [6].

## 5. Conclusions

We have shown that the transport and thermodynamic quantities can be written simply in terms of a single function, the spectral function, which is related to the return probability for a diffusive particle. This function is determined by the geometry of the system and the magnetic field. Once it is calculated, all physical quantities can be deduced immediately.

## References

1. Büttiker M, Imry Y, Landauer R *Phys. Lett. A* **96** 365 (1983)
2. Lévy L P et al. *Phys. Rev. Lett.* **64** 2074 (1990); Reulet B et al. *Phys. Rev. Lett.* **75** 124 (1995)
3. Chandrasekhar V et al. *Phys. Rev. Lett.* **67** 3578 (1991)
4. Mailly D, Chapelier C, Benoit A *Phys. Rev. Lett.* **70** 2020 (1993)
5. Mohanty P et al., in *Quantum Coherence and Decoherence* (Eds K Fujikawa, Y A Ono) (Amsterdam, New York: Elsevier/North Holland, 1996) p. 191
6. Montambaux G, in *Quantum Fluctuations, Ecole d'été de physique théorique, Les Houches, Session LXIII 27, juin–28 juillet 1995* (Eds S Reynaud, E Giacobino, J Zinn-Justin) (Amsterdam, New York: Elsevier, 1997) p. 387
7. Cheung H-F, Riedel E K, Gefen Y *Phys. Rev. Lett.* **62** 587 (1989)
8. Von Oppen F, Riedel E K *Phys. Rev. Lett.* **66** 84 (1991); Altshuler B L, Gefen Y, Imry Y *Phys. Rev. Lett.* **66** 88 (1991); Akkermans E *Europhys. Lett.* **15** 709 (1991)
9. Schmid A *Phys. Rev. Lett.* **66** 80 (1991)
10. Oh S, Zyuzin A Yu, Serota R A *Phys. Rev. B* **44** 8858 (1991)
11. Argaman N, Imry Y, Smilansky U *Phys. Rev. B* **47** 4440 (1993)
12. Ambegaokar V, Eckern U *Phys. Rev. Lett.* **65** 381 (1990)
13. Argaman N, Imry Y *Phys. Scr.* **T49** 333 (1993)
14. Montambaux G *J. Phys. I (Paris)* **6** 1 (1996)
15. Pascaud M, Montambaux G *Europhys. Lett.* **37** 347 (1997); Pascaud M, Montambaux G *Proc. Minerva Workshop on Mesoscopic, Fractals and Neural Networks*, to appear in *Phil. Mag.* (1997) (in press)
16. Khmel'nitskii D E *Physica B* **126** 235 (1984)
17. Doucot B, Rammal R *Phys. Rev. Lett.* **55** 1148 (1985); *J. Phys. (Paris)* **47** 973 (1986)
18. Argaman N *Phys. Rev. B* **53** 7035 (1996)
19. Eckern U *Z. Phys. B* **82** 393 (1991)
20. Andreev A V, Altshuler B L *Phys. Rev. Lett.* **75** 902 (1995)
21. Altshuler B L, Aronov A G, in *Electron-Electron Interactions in Disordered Systems* (Modern Problems in Condensed Matter Sciences Vol. 10, Eds A L Efros, M Pollak) (Amsterdam: North-Holland, 1985) p. 1

22. Al'tshuler B L, Shklovskii B I *Zh. Eksp. Teor. Fiz.* **91** 220 (1986) [*Sov. Phys. JETP* **64** 127 (1986)]  
 23. Maily D et al., in *Quantum Coherence in Mesoscopic Systems* (NATO ASI Series B Vol. 254, Ed. B Kramer) (New York: Plenum Press, 1991) p. 401  
 24. Aronov A G, Sharvin Yu V *Rev. Mod. Phys.* **59** 755 (1987)

## Electrons in quasi-one-dimensional conductors: from high-temperature diffusion to low-temperature hopping

M E Gershenson, Yu B Khavin, A L Bogdanov

### 1. Introduction

The past two decades have seen spectacular progress in the physics of low-dimensional disordered conductors [1, 2]. One of the directions of rapid growth is the study of electron transport in quasi-one-dimensional (1D) conductors. The experimental study of this problem is crucial for our understanding of transport mechanisms in a diversity of 1D systems: metal-film and semiconductor nanometer structures [3], heavy-doped conjugated polymers [4], carbon nanotubes [5], and many others.

It is widely believed that all electron states in low-dimensional conductors are localized [6, 7], at least in the case of weak electron–electron interaction. The extent of the electron wavefunction is characterized by the localization length  $\xi$ ; for a quasi-1D conductor,

$$\xi = \frac{\pi\hbar}{e^2} \frac{W}{R_{\square}} = 2\pi\hbar v_{2D} D W, \quad (1)$$

where  $v_{2D}$  is the two-dimensional (2D) density of electron states,  $D$  is the electron diffusion constant, and  $W$  is the width of a thin-film ‘wire’. In quasi-one-dimensional conductors, the largest cross-sectional dimension is smaller than  $\xi$ , and, at the same time, is much greater than the wavelength of the current carriers. In spite of localization, the conductivity of 1D conductors can be very high at room temperature. This ‘metallic’ conductivity is due to the strong inelastic scattering: the electron scatters to another state, localized around a different site, before it diffuses over the localization length. This is the weak localization (WL) regime. However, with decreasing temperature, a 1D conductor will inevitably become an insulator. Electron transport could proceed by hopping only in this strong localization (SL) regime.

The goal of this work is an observation of the crossover between WL and SL regimes and experimental study of electron transport on the insulating side of the crossover.

### 2. Crossover from weak to strong localization

The theoretical prediction of the crossover from diffusion to hopping in 1D conductors with decreasing temperature was made by Thouless [6] in 1977. However, the experimental study of this fundamental problem was delayed for 20 years. The ‘gap’ between the prediction and observation indicates that this is a very demanding experiment; in particular, the choice of adequate samples is important for success. Recently we observed the crossover as a function of temperature in experiments with narrow channels in the MBE-grown Si  $\delta$ -doped GaAs structures [8]. The samples consisted of single

sheets of Si donors with concentration  $(3-5)\times 10^{12}$  cm $^{-2}$ , which were 0.1  $\mu$ m below the surface of an undoped GaAs. Using the e-beam lithography and ion etching, we were able to prepare uniform conducting channels of effective width  $W$  as narrow as 0.05  $\mu$ m. (Because of the side depletion, the effective width is smaller than the geometrical width by 0.15–0.2  $\mu$ m, depending on the concentration of carriers). In order to reduce the effect of mesoscopic conductance fluctuations, we made these wires long enough (the length  $L = 40-500$   $\mu$ m was much greater than the localization length) and connected many wires in parallel (up to 500 wires). Parameters of several samples are listed in Table 1.

**Table 1.** Parameters of the samples.

Sample	1	2	3	4	5	6
$W$ , $\mu$ m	0.05	0.06	0.1	0.12	0.2	0.18
$L$ , $\mu$ m	500	500	40	500	40	500
No. of parallel ‘wires’	470	470	5	470	5	470
$R_{\square}(T = 20\text{ K})$ , k $\Omega$	1.6	1.7	3.5	1.6	4.2	1.7
$\xi$ , $\mu$ m	0.40	0.46	0.37	1.0	0.61	1.4
$\Delta_{\xi}$ , K	2.1	1.5	1.1	0.35	0.34	0.17
$T_0(H = 0)$ , K	2.6	1.87	1.47	0.42	0.39	0.2
$R_{\xi}(T = T_0)$ , k $\Omega$	20.4	21.3	28	23	24.4	24.3
$H_{\xi}$ , kOe	1.0	0.74	0.56	0.17	0.17	0.083
$H_{\xi}^{\text{exp}}$ , kOe	1.0	0.80	0.51	0.21	0.17	0.12
$H_{\xi}^{\text{exp}}/T_0$ , kOe K $^{-1}$	0.37	0.43	0.35	0.50	0.44	0.59

The mean free path of electrons is small in the  $\delta$ -doped layers (17–35 nm) because of the strong scattering of electrons by ionized impurities, and the electron motion is always diffusive at distances smaller than the wavefunction envelope of the length  $\xi$ . The relatively high concentration of carriers ensures that the number of occupied 1D sub-bands  $N_{1D} = k_F W/\pi$  is large;  $N_{1D} \simeq 7$  even in the narrowest sample 1. However, with respect to the quantum interference effects all the samples are one-dimensional at low temperatures [ $W < \xi$ ,  $L_{\varphi}(T)$ ].

The resistance of the samples increases with decreasing temperature (Fig. 1); a slow growth of  $R$  (logarithmic above 10 K) is consistent with the theory of quantum corrections to the resistance in the WL regime [8]. However, below a certain crossover temperature, a dramatic change in the dependence  $R(T)$  was observed: it becomes exponentially strong and can be fit with an activation law

$$R(T) = R_0 \exp\left(\frac{T_0}{T}\right). \quad (2)$$

The Arrhenius-type dependence (2) was observed for all the samples at  $T \leq 0.3T_0$ , where  $T_0$  is the temperature that corresponds to the activation energy (see Fig. 1). The crossover from the one-dimensional WL dependence  $R(T)$  to a stronger one occurs at  $T \approx T_0$ ; below we identify the crossover temperature with  $T_0$ .

The proof that we observe the Thouless crossover from weak to strong localization is based on two experimental facts. Firstly, the resistance  $R_{\xi}$ , calculated for a wire segment of length  $\xi$  at  $T = T_0$ , turns out to be  $24 \pm 4$  k $\Omega$  for different samples (see Table 1); this is consistent with the resistance  $\sim h/e^2$  expected for a 1D conductor of length  $\xi$  in the vicinity of the crossover [6]. Secondly, in terms of competition between the length scales, the crossover should occur when the temperature-dependent length  $L_{\varphi}(T)$  becomes compar-